EMC impact on the RPW science performance in space

RPW-SCI-TSR-001894-LES
Iss. 1, Rev. 0

Prepared and approved after verification by	Function:	Signature:	Date
The RPW Team		Signature numérique de Milan Maksimovic Date : 2020.10.21 12:14:41 +02'00'	16/10/2020
Verified by:	**Function:**	**Signature:**	**Date**
For application:	**Function:**	**Signature:**	**Date**

CLASSIFICATION **PUBLIC** ☒ **RESTRICTED** ☐

l'Observatoire de Paris — LESIA
Laboratoire d'Études Spatiales et d'Instrumentation en Astrophysique

CNRS-Observatoire de PARIS
Section de MEUDON – LESIA
5, place Jules Janssen
92195 Meudon Cedex – France

Change Record

Issue	Rev.	Date	Authors	Modifications

Acronym List

Acronym	Definition	Acronym	Definition
BIAS	Biasing Unit	MEB	Main Electronic Box
CNES	Centre National d'Etudes Spatiales	RPW	Radio & Plasma Waves instrument
EMC	Electro Magnetic Cleanliness	TDS	Time Domain Sampler
ESA	European Space Agency	TNR-HFR	Thermal Noise Receiver- High frequency receiver
LFR	Low Frequency Receiver		

Table of Contents

1 GENERAL

1.1 Scope of the Document

This document describes the EMC impact on the RPW science performance in space. The strongest EMC perturbations on RPW are mostly due to the poorly designed Solar Orbiter platform. At the time of writing this report it seems that there are no obvious possible mitigations of these EMC pollutions on the spacecraft side. We therefore present also the necessary mitigations which we could implement on RPW.

1.2 Reference Documents

This document is based on the documents listed in the following table:

Mark	Reference/Iss/Rev	Title of the document	Authors	Date
RD1	RPW-SYS-SOW-001518-LES, Iss. 2, Rev. 1	RPW Science Performances	M. Maksimovic	15/05/2020
RD2	SOL.S.ASTR.MN.00649	Minutes of the EMC Meeting Working Group Meeting #6		6/7 June 2013

2 THE EMC PERTURBATIONS OBSERVED BY RPW

In this section we describe the EMC impact on the RPW science performance in space. We have decided to divide this section according to the RPW MEB subsystems.

2.1 Perturbations of the TNR-HFR

2.1.1 Magnetic

Magnetic power spectra measured by TNR shows a major perturbation at around the 120kHz coming from the PCDU (Power Converter and Distribution Unit) and being radiated by the solar panels. Although the amplitude of this perturbation changes in time (see the following section) it is always present in the TNR magnetic data. Another perturbation, not always present but occurring regularly in time, is detected at the two frequencies of 244.6 and 255.5 kHz.
Figure 2.1.1 shows the magnetic dynamic spectra measured by TNR on three different days. The perturbation line at 120kHz is visible in the data along with the perturbation at high frequency occurring at some regular times. The amplitude and the frequency of occurrence of the high frequency perturbation on the magnetic signal vary in time.

This is clearly visible in the time evolution of the magnetic spectral power at 244.6 and 255.5 kHz and the corresponding Fourier Transforms (FT) of these signals, displayed on Figure 2.1.2. The occurrence and the periodicity of the regular peaks in the initial magnetic signals, as well as the amplitudes of their FT peaks change for the 3 displayed data samples. The amplitude of the interference is higher on May 7th and it almost disappear in the September data. The frequency of occurrence increases from May 2th to 7th.

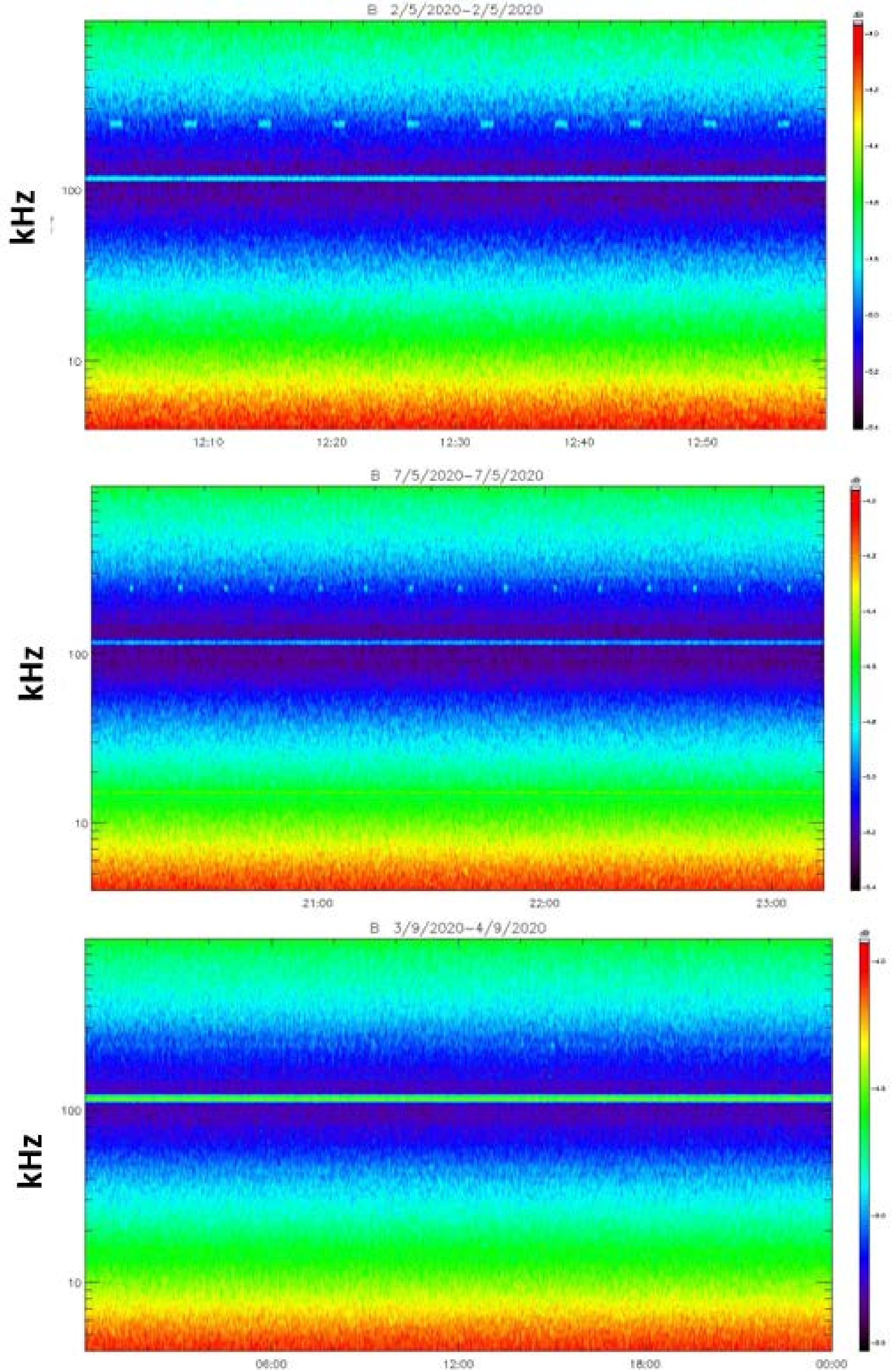

Figure 2.1.1: *Magnetic power spectral density measured by TNR on 02/052020 (upper panel), on 07/05/2020 (middle panel) and on 03/09/2020 (lower panel).*

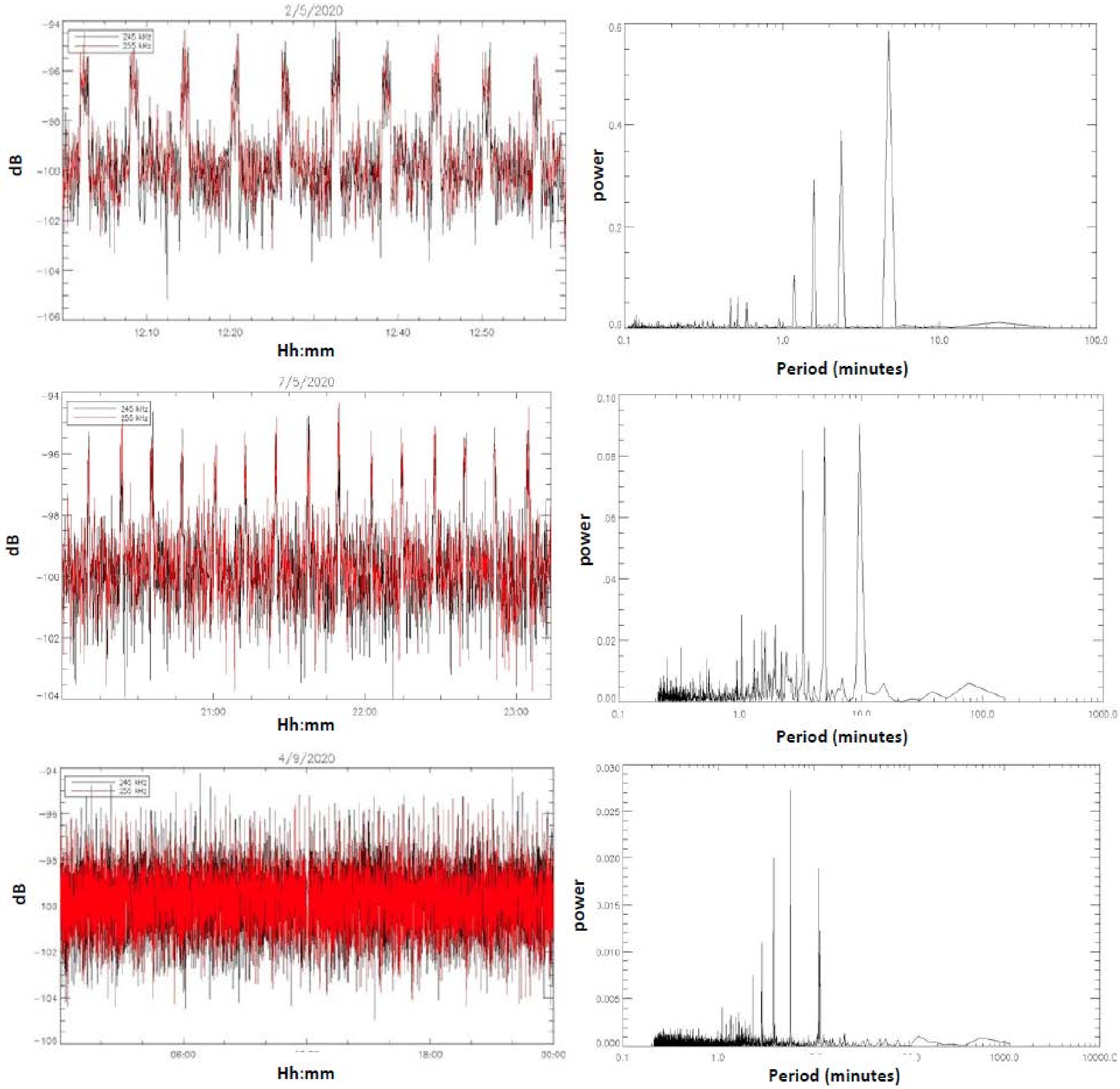

Figure 2.1.2: *Time evolution of the magnetic power at the TNR frequencies of 244.6 and 255.5 kHz (left panels). Fourier Transforms of the 244.6 kHz signal (right panels). The same three days as on Figure 2.1.1 are displayed: 02/052020 (upper panels), 07/05/2020 (middle panels) and 03/09/2020 (lower panels).*

A possible origin of the high frequency interference can be the MAG heater that operates at a frequency of 262 kHz. The varying amplitude and the changing frequency of occurrence can depend on the periods in which the heater is on, depending on the distance from the Sun.

2.1.2 Electric

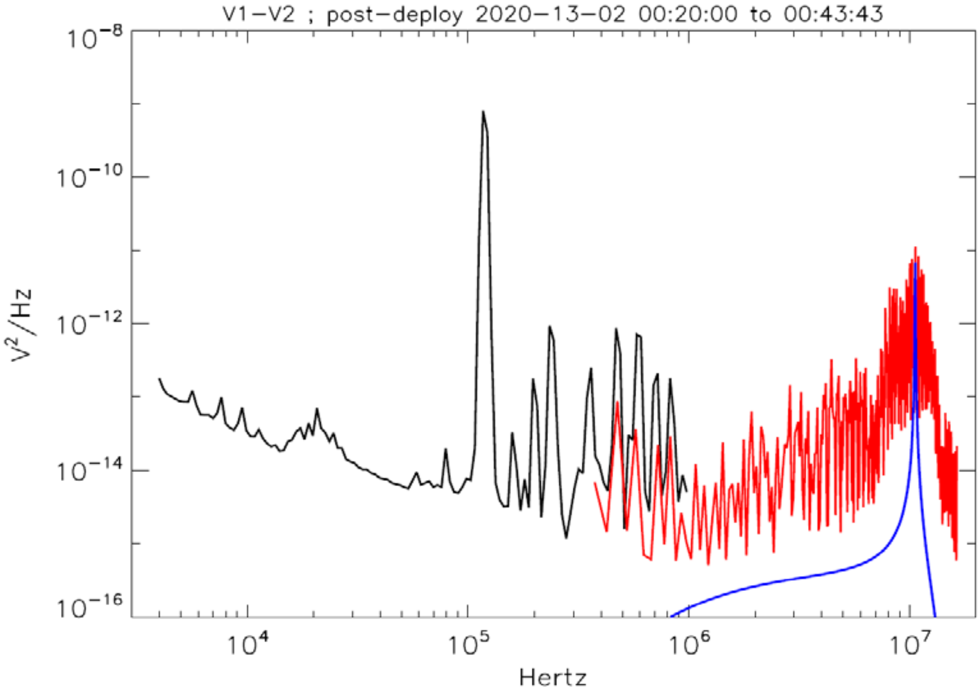

Figure 2.1.3

Figure 2.1.3 displays the main EMC pollution on the TNR-HFR measurements caused by the Solar Orbiter platform. These pollutions are due to

- The 80 kHz coming from the RW (Reaction Wheels) electronic box
- The many lines (maximum of 6) around the 120kHz coming from the PCDU (Power Converter and Distribution Unit) and being radiated by the solar panels

On Figure 2.1.4 we display how the fundamental and harmonic emissions of these two spurious are polluting most of the TNR frequency range above 80 kHz.

At higher frequencies, in HFR, the many harmonics of these frequencies create a background of spurious lines which pollute the whole spectrum, as can be seen on the red curve of Figure 2.1.3. On this Figure a model of the galactic radio background, as it should be seen by the RPW antennas, is indicated by the blue curve. Only a few HFR frequencies are close to this background.

Several other EMC pollutions are also visible on the TNR spectra below 80 kHZ. These pollutions are variables both in frequency and amplitude. The root cause of these is still under investigation.

Finally, a periodic signal at around 300 kHz, which is due to the S/C battery charging is observed starting on June 06 2020 @ 00:34. This perturbation can be seen on Figure 3.1.1. According to the ESA project, this perturbation should be minimized in the future.

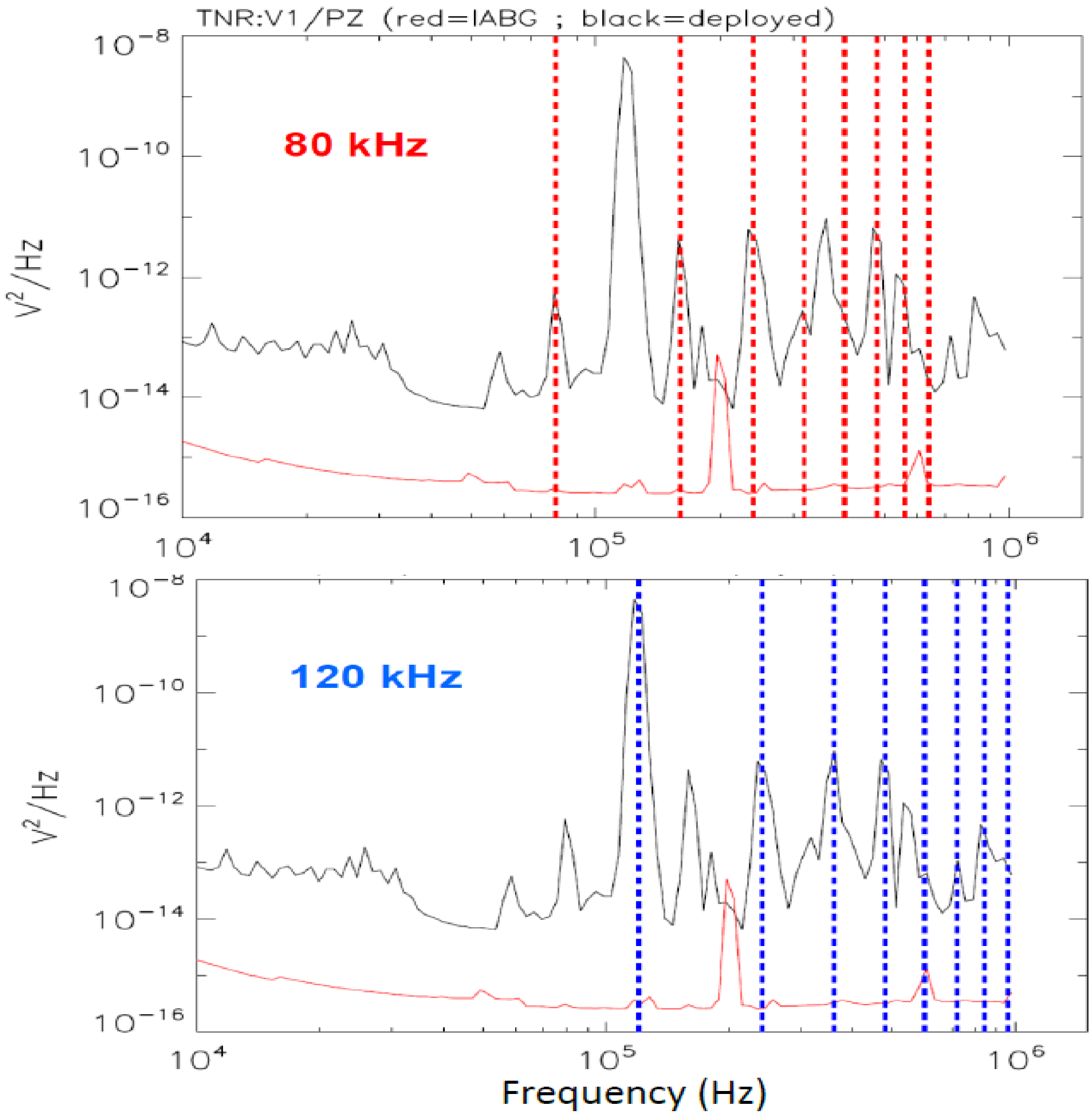

Figure 2.1.4

2.2 Perturbations of the TDS

2.2.1 Magnetic

TDS only samples the B_MF channel of SCM, effective between 100 kHz and ~220 kHz. The Figure 2.2.1 below shows TDS magnetic spectrum (spectrum of voltage at TDS input without the sensor transfer function applied) with all the typical interference lines. Here TDS was in the more sensitive high gain mode. The spectrum is calculated from time domain data sampled at 524 kHz with 8192 point FFT.

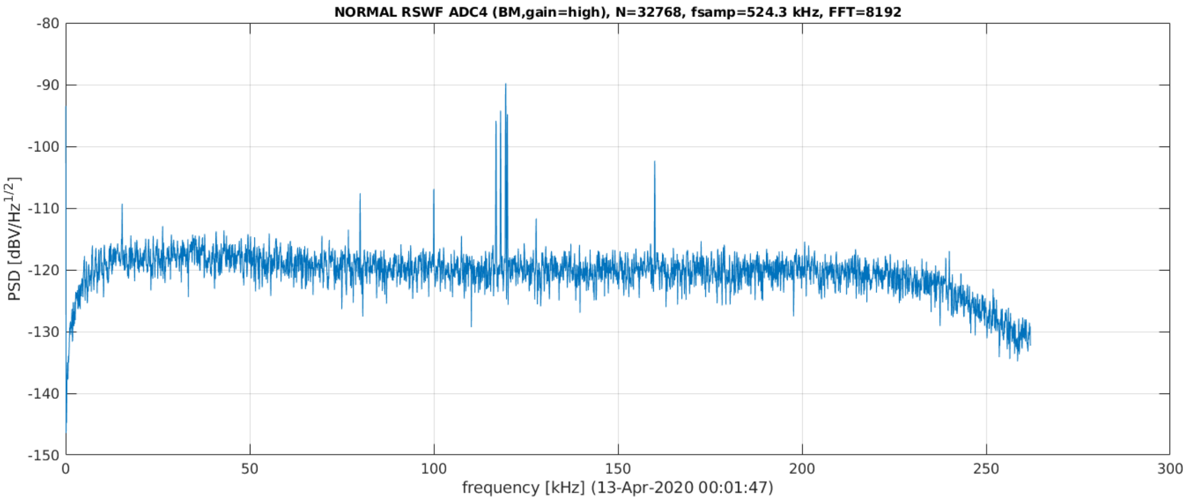

Figure 2.2.1

The background level is the noise floor of the SCM magnetic sensor. In the spectrum, we observe multiple interference lines:

- The strongest perturbation, up to 30 dB above noise floor is the spacecraft PCDU emission with multiple spectral lines between 117 and 120 kHz (the character is the same as for electric field, as described below).
- 80 kHz and 160 kHz interference lines, probably originating from the reaction wheels. These are very stable and narrowband.
- 5.3 kHz MAG drive frequency.
- 100 kHz emission, most likely emitted from the RPW power supply.

Apart from the PCDU, all the other lines are relatively weak, stable and narrowband in frequency.

2.2.2 Electric

TDS samples the signal from the three electric antennas either in monopole mode or in dipole mode (digitizing differential voltages) in the frequency band from 100 kHz and ~220 kHz. The Figures 2.2.2 & 2.2.3 below show TDS electric field spectra, with effective antenna length assume to be 1m, showing all the typical interference lines. Here TDS was in the more sensitive high gain mode. The spectrum is calculated from time domain data sampled at 524 kHz with 8192 point FFT.

The following interference is observed in monopole mode :

- The strongest perturbation, up to 60 dB above noise floor is the spacecraft PCDU emission with multiple spectral lines between 117 and 121 kHz. Harmonics of that emission are also observed. This emission is present, but reduced by about 10 dB in dipole mode.
- 80 kHz and 160 kHz interference lines, probably originating from the reaction wheels. These are very stable and narrowband.
- A set of harmonics spaced by about 2.2 kHz seen below 40 kHz and around 80 kHz.
- 200 kHz emission, most likely emitted from RPW BIAS power supply.
- Emission around 127 kHz.
- Variety of other weaker emissions.

Notably, many of the emissions disappear in dipole mode (Figure 2.2.3) due to the common mode rejection of the instrument and the remaining ones are weaker. Only the following remain in dipole mode :

- The strongest perturbation, up to 50 dB above noise floor is still the spacecraft PCDU emission with multiple spectral lines between 117 and 121 kHz.
- 80 kHz and 160 kHz interference lines remain, but with a lower amplitude. Sometimes, the disappear completely.
- 200 kHz emission, most likely emitted from RPW BIAS power supply.
- 127 kHz line remains, but with a low amplitude.

Figure 2.2.4 shows a detail of the PCDU spike cluster. Between 5 and 6 individual spikes can be distinguished, which are relatively stable in frequency and vary in amplitude by up to 15 dB in time.

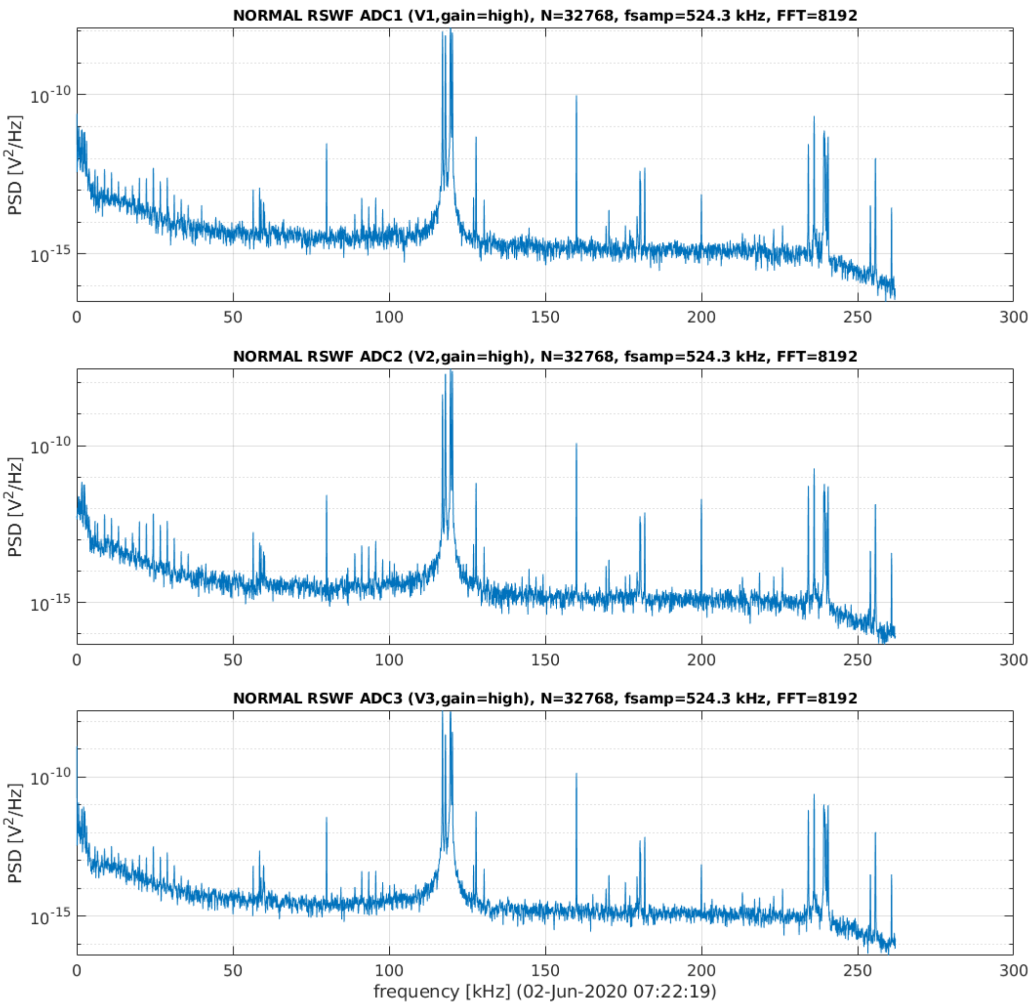

Figure 2.2.2 : *TDS spectrum in monopole mode, where each TDS channel measures antenna voltage against spacecraft ground.*

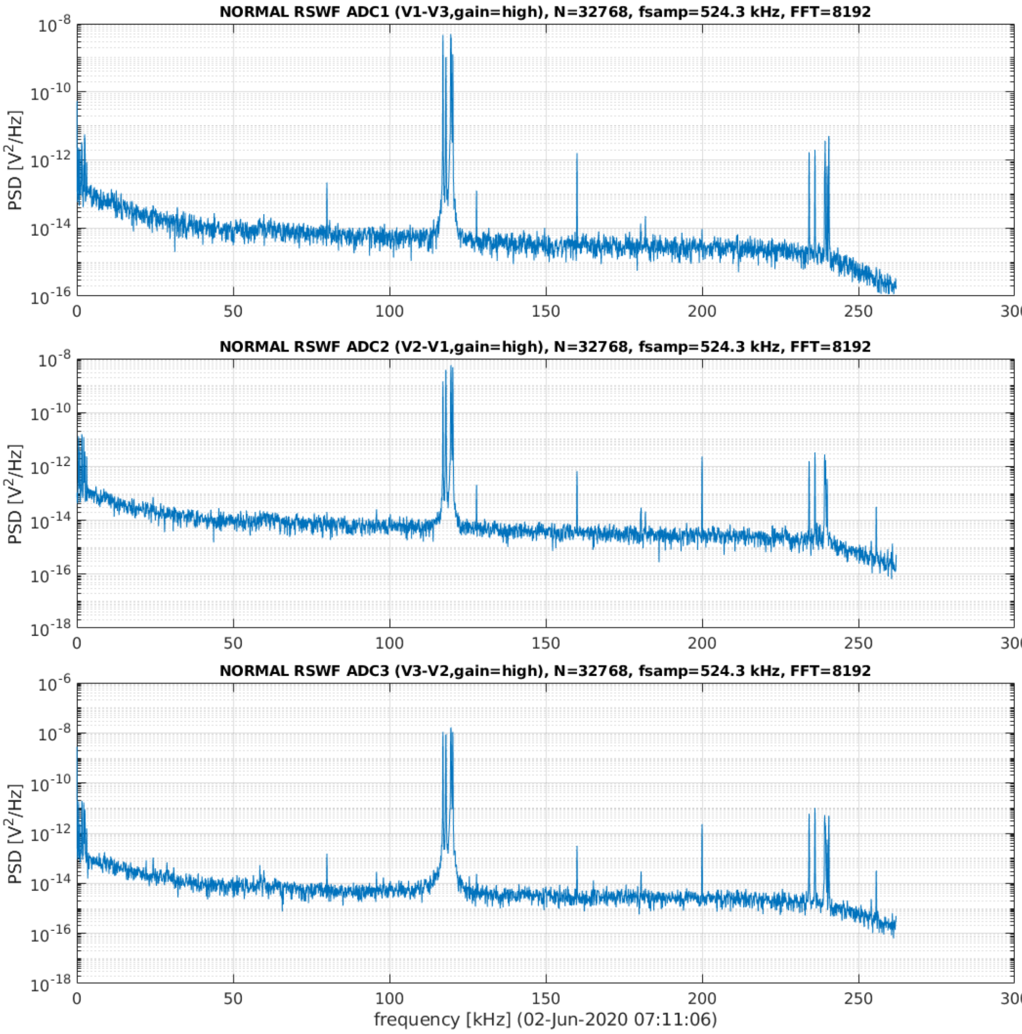

Figure 2.2.3 *TDS spectrum in dipole mode, where each TDS channel measures differential voltage between a pair of antennas.*

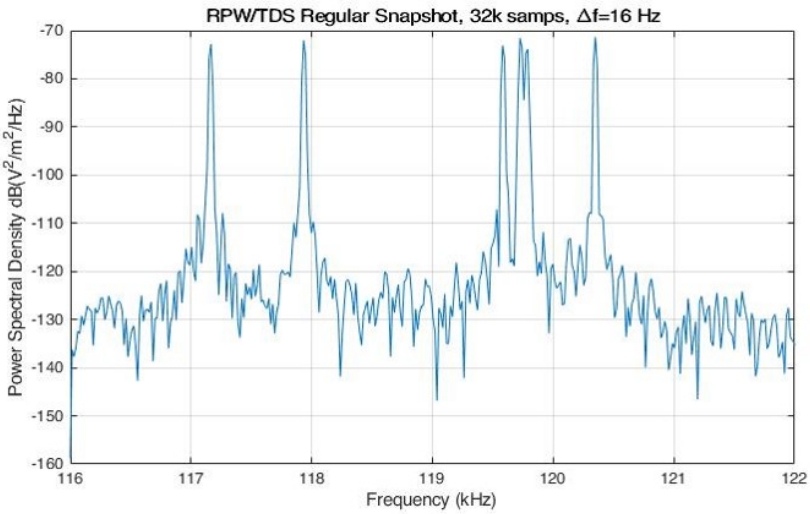

Figure 2.2.4 *A detail of the PCDU interference with a fine resolution (16 Hz bandwith)*

2.3 Perturbations of the LFR

2.3.1 Magnetic

On Figure 2.3.1 a regular broadband perturbation in the LFR-F1 frequency range is observed every ~ 3h. At this stage the precise origin of this perturbation is unclear. For instance, we do not understand why this perturbation is not visible on the Snapshot Waveform (SWF) data. Is this perturbation self-induced by the LFR operation itself? Is it due to the platform? This topic is still under investigation.

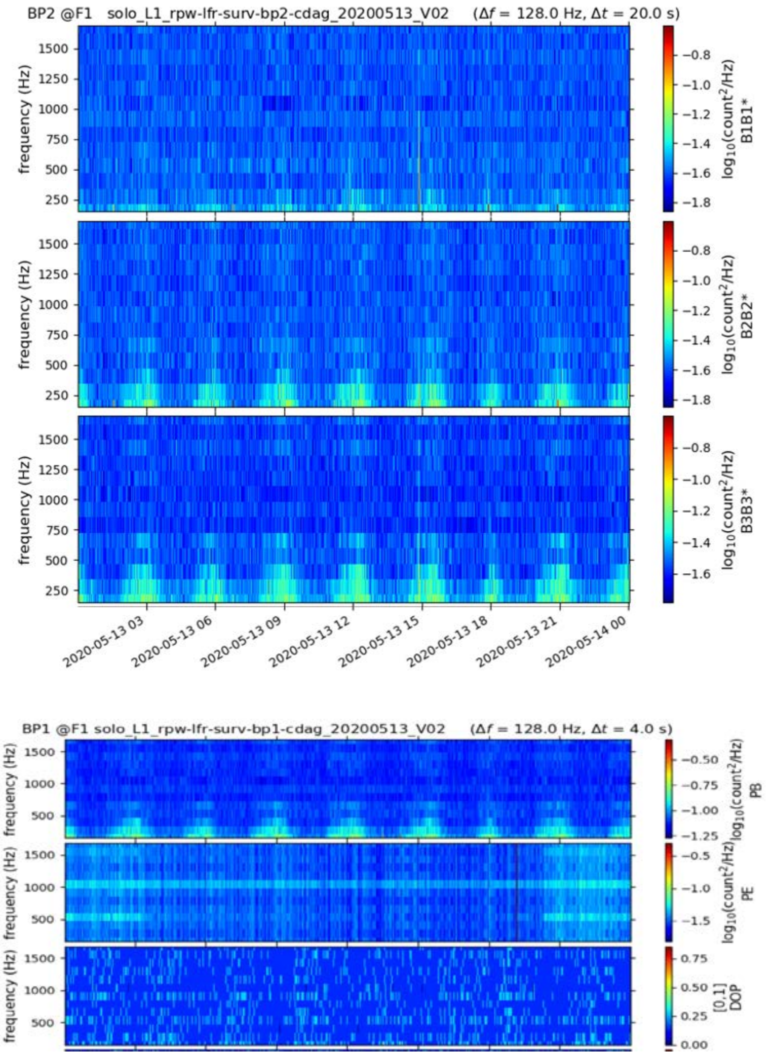

Figure 2.3.1

Note that this ~3 hours' perturbations are sometime enhanced as can be seen on Figure 2.3.2. Paradoxically, and as already mentioned above, this perturbation does not seem to be observable on the Snapshot Waveforms as can be seen on Figure 2.3.3.

In addition, a weak spectral line is also regularly observable at ~1000Hz (more faintly at ~200Hz), see Figure 2.3.4

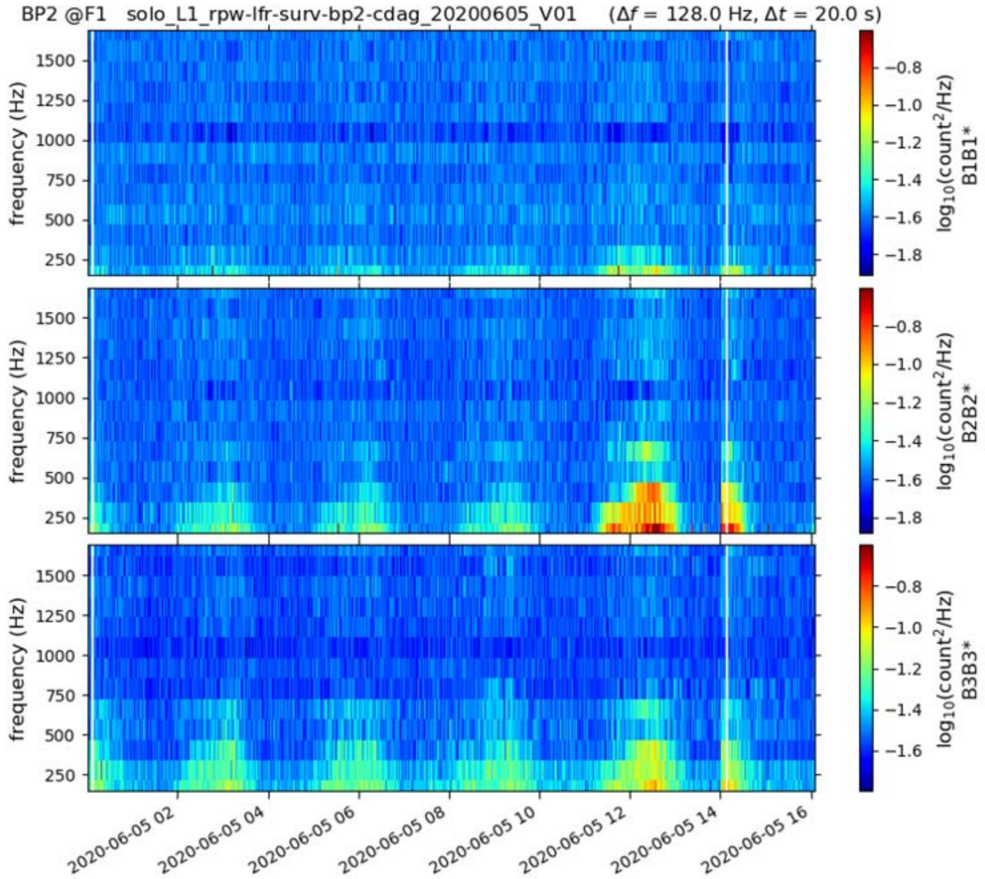

Figure 2.3.2

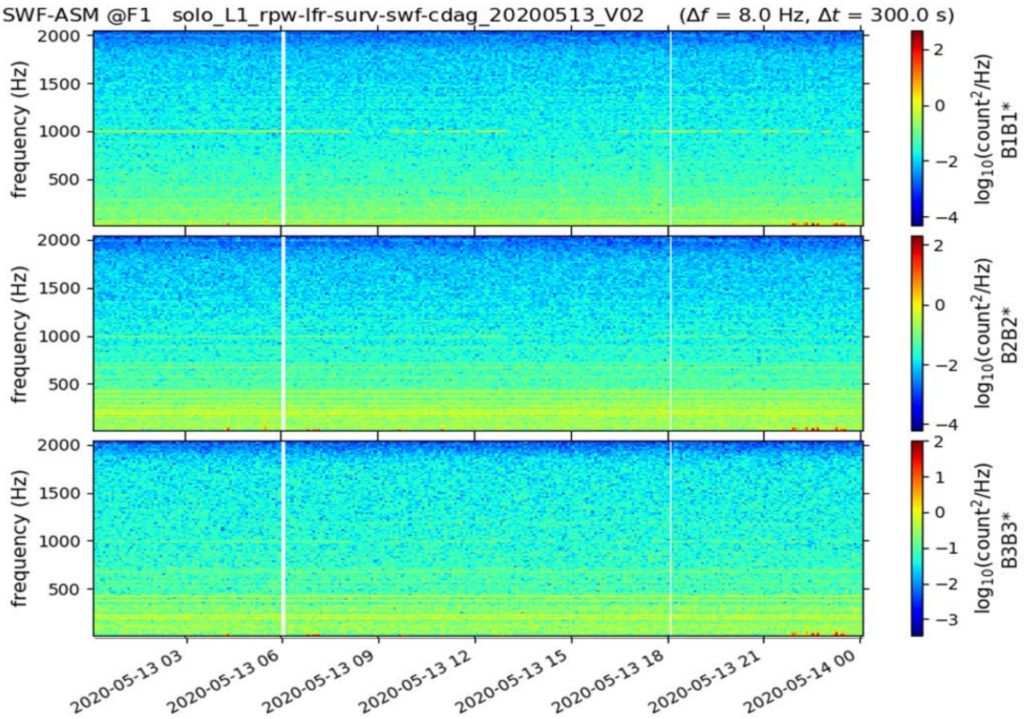

Figure 2.3.3

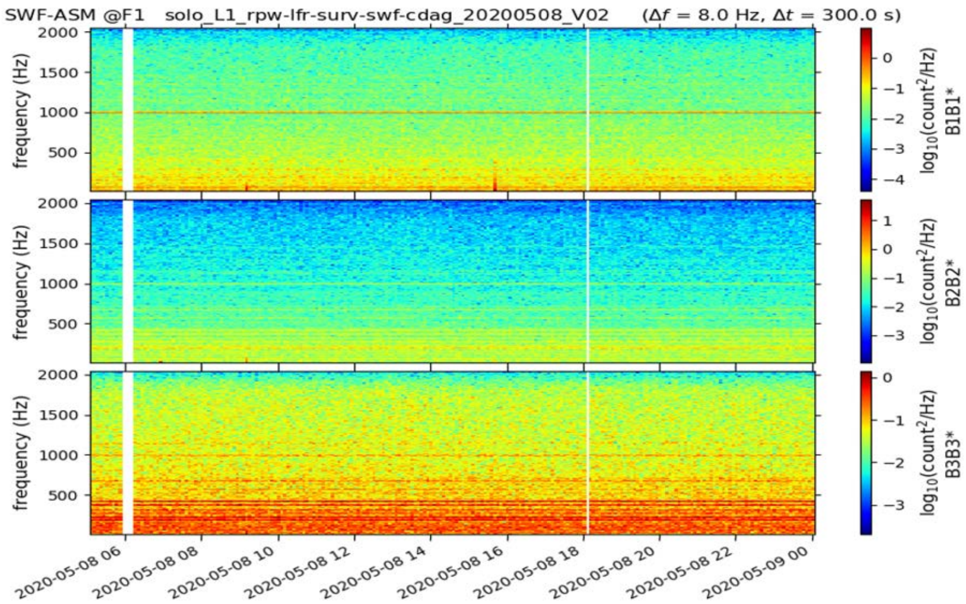

Figure 2.3.4

At the F2 frequency range, as can be seen on Figure 2.3.5, there are two 8Hz and 16Hz lines and their harmonics originating from the AOCS Synchronization Pulse (ASP). They are well observable from the waveform products (SWF, CWF). Their magnitudes are relatively weak at low frequency but surprisingly increase at higher frequencies, where the signal can be seen up to several kHz. There are also two peaks at 1.33Hz and 2.66Hz whose origin is unclear (might be EUI heater but this is to be confirmed).

The 8Hz and 16Hz are hardly observable from the onboard spectral products (ASM, BP2, BP1) since the digital sensitivity of the onboard FFT is less than the waveform one's. See Figure 2.3.6.

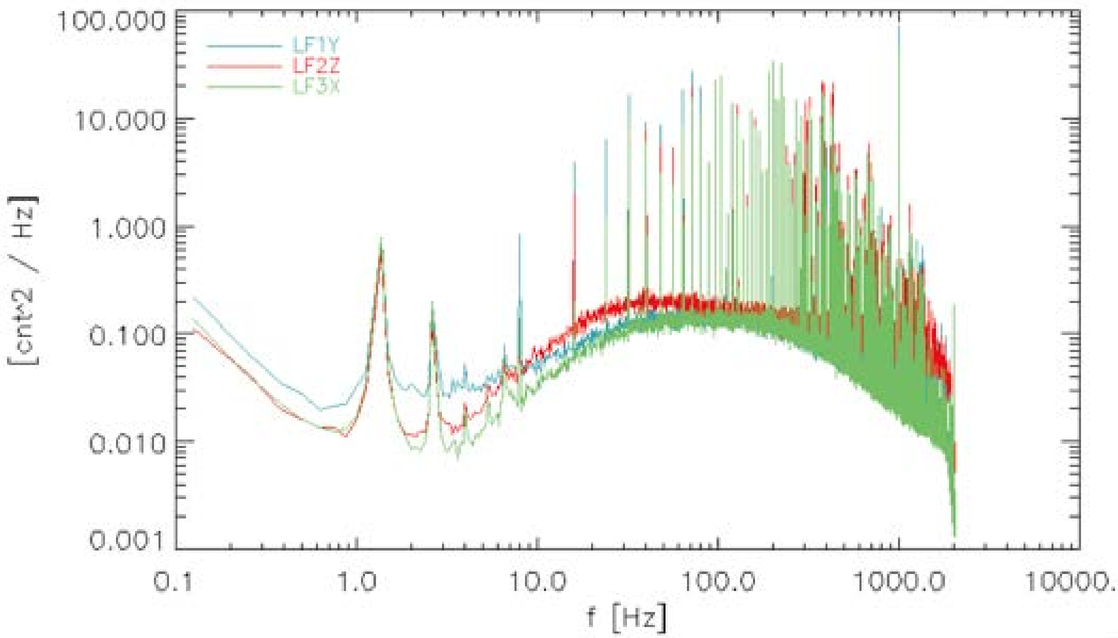

Figure 2.3.5

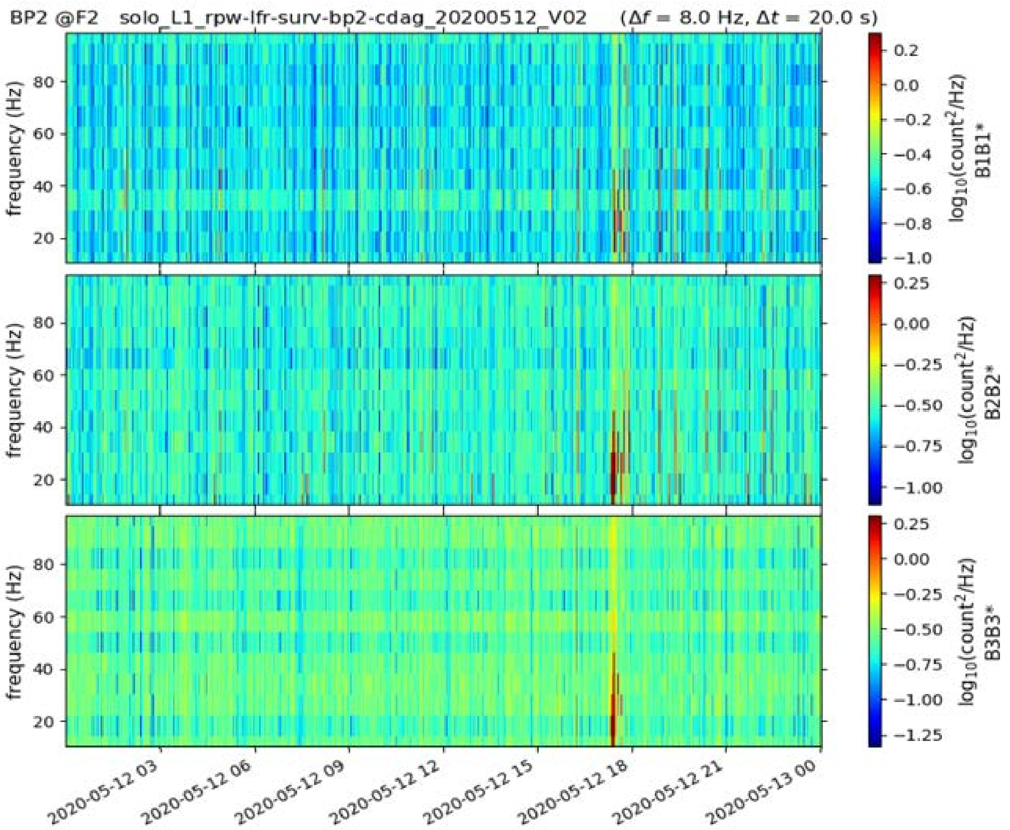

Figure 2.3.6

There are also more or less regular spikes, every about 90s depending on the need to heat SCM, that originates from the SCM heater switch on or off. The effects stand for 0.1 to 0.2 s but affect all frequencies. See Figure 2.3.7

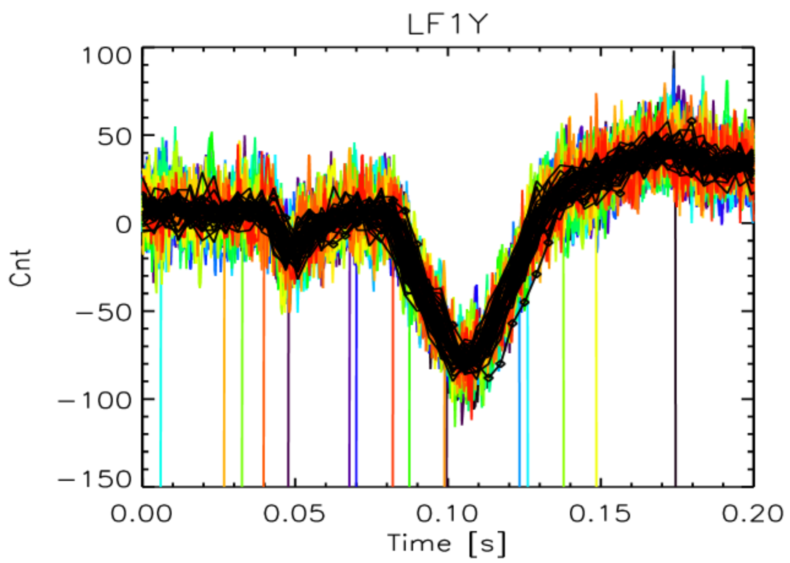

Figure 2.3.7 : *Zoom on the SCM heater signature on the LF1Y antenna. Each color corresponds to one observation. Vertical lines are caused by the plot and are not signal variations.*

At the F0 frequency range no specific perturbation except the ~1000Hz line already noticed at F1. See Figure 2.3.8.

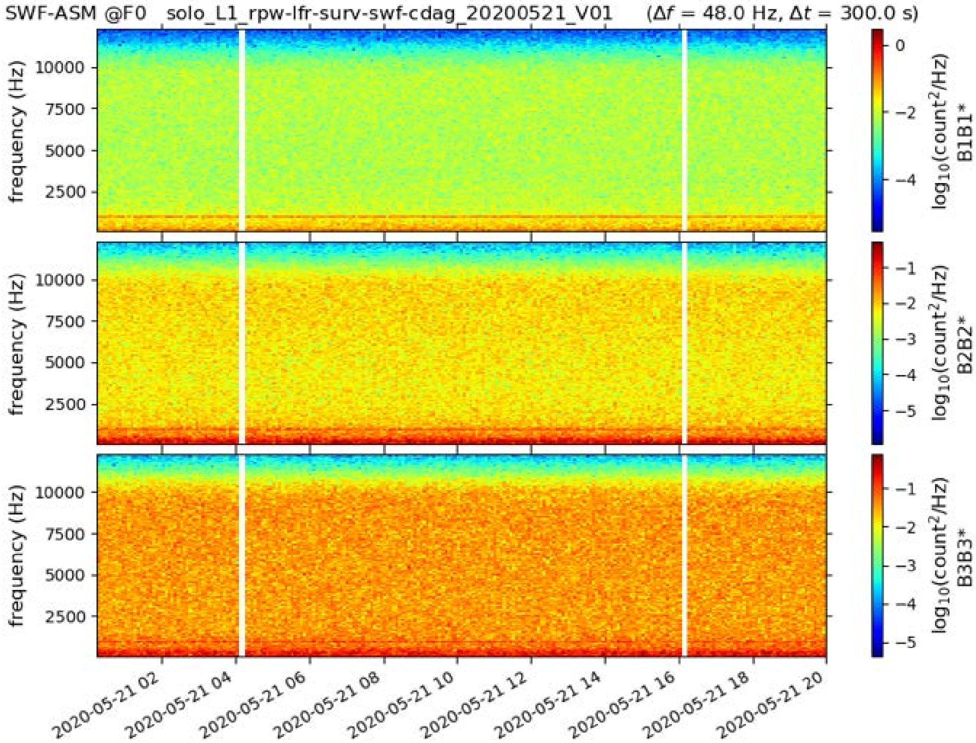

Figure 2.3.8

At the beginning of the mission a spectral line at ~6300Hz was also clearly observable. This line is due to Solo-HI, as also observed during the EMC campaign on 2-3 June 2020 (see section 2.6). Furthermore, broadband noise/harmonics up to 3000Hz have also been observed when EUI was in EMC Mode 2 (IU_EMC-3-16-mode-2), see Figures from section 2.6.

2.3.2 Electric

The BIAS instrument is less noisy than the SCM. The digital noise of the waveform is therefore often observed. However, the electric spectrograms showed some faint curved moving lines. Such spectral features were already observable on ground. They are believed to be caused by the SpaceWire activity, due to the small distance between the SpaceWire connector and the ADC bus in the LFR PCB.

Other spectral lines are observed, which seem not to be caused by LFR. In particular, a double line between 1000Hz and 1500Hz, which is well observable on the monopole measurement V but also on the differential measurements E1 and E2, has been observed from the beginning of the mission, although not at a fixed place in the frequency range.

Another spectral line is also regularly present at ~36Hz and its third harmonic. This latter is moving. For instance, at the beginning of the mission it was at ~33Hz. See *Figure 2.3.9.* Actually this specific spectral line (and harmonics) has became more and more ennoying since the beginning of the mission because its intensity has increased. For instance, it is now clearly visible from the onboard spectral products as displayed on Figures 2.3.10 and 2.3.11. Its origin is still unknown but in Figure 2.3.12, one can very likely see when and how it appears.

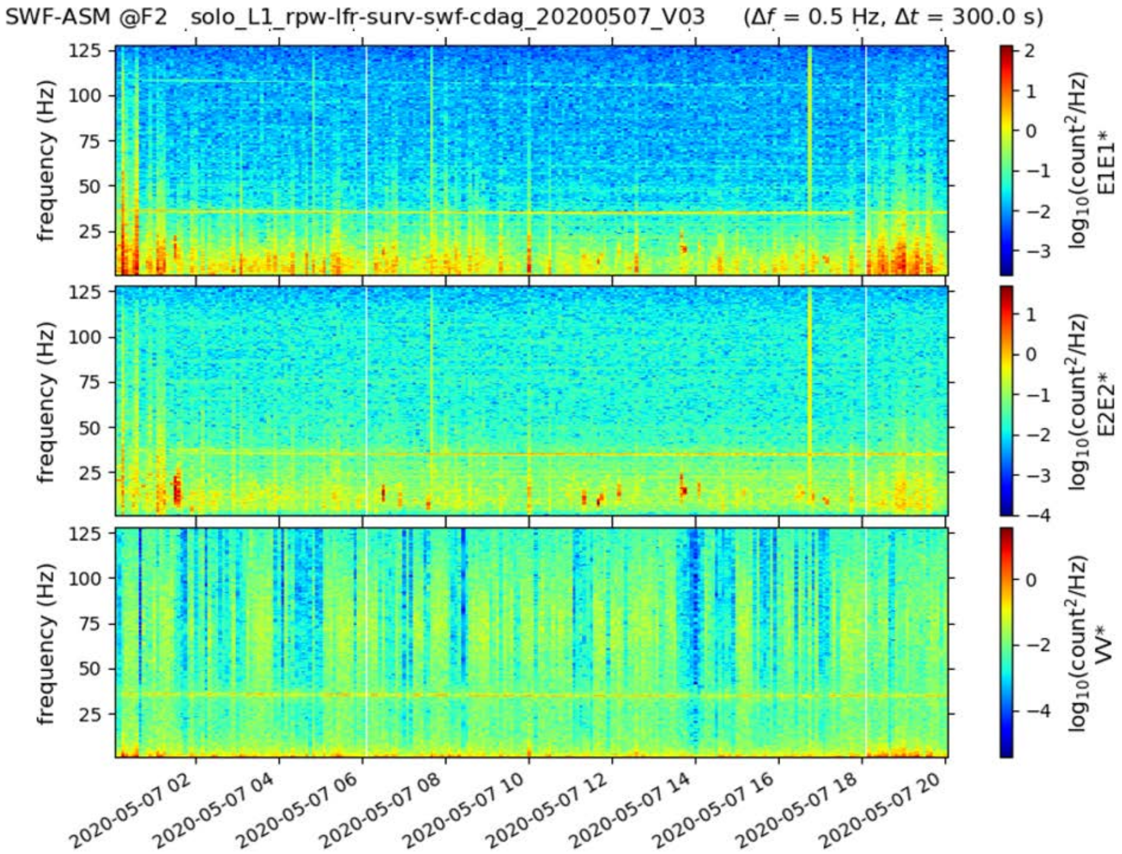

Figure 2.3.9

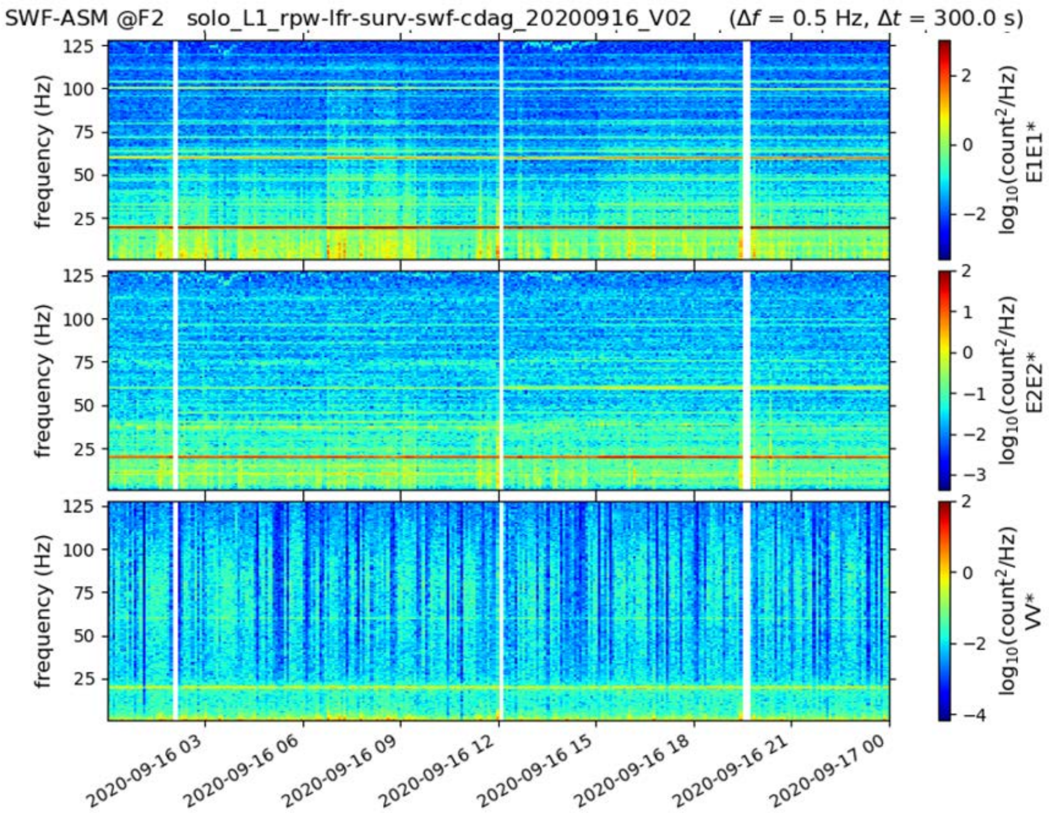

Figure 2.3.10

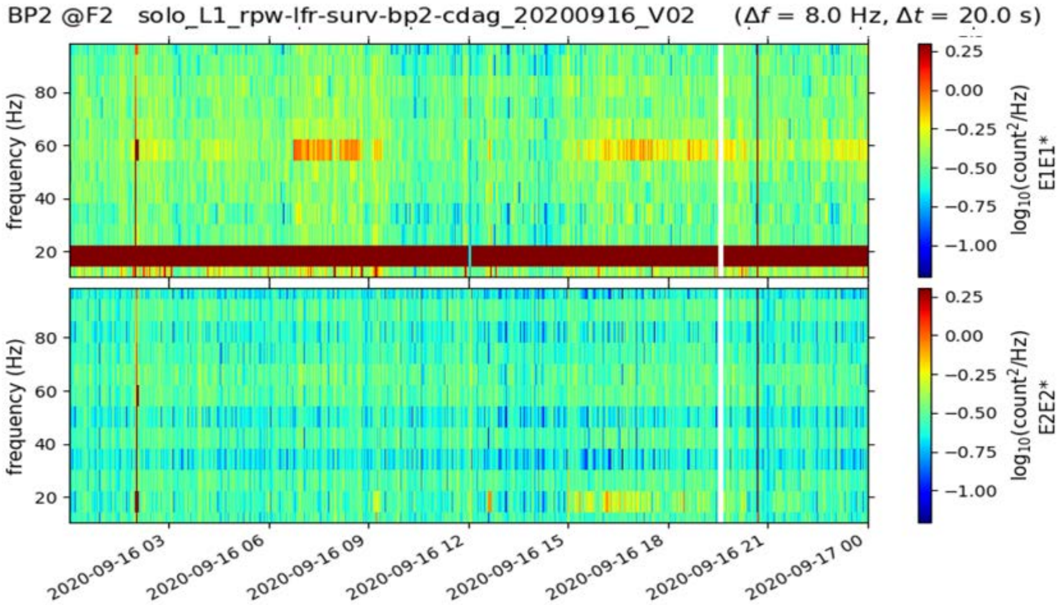

Figure 2.3.11

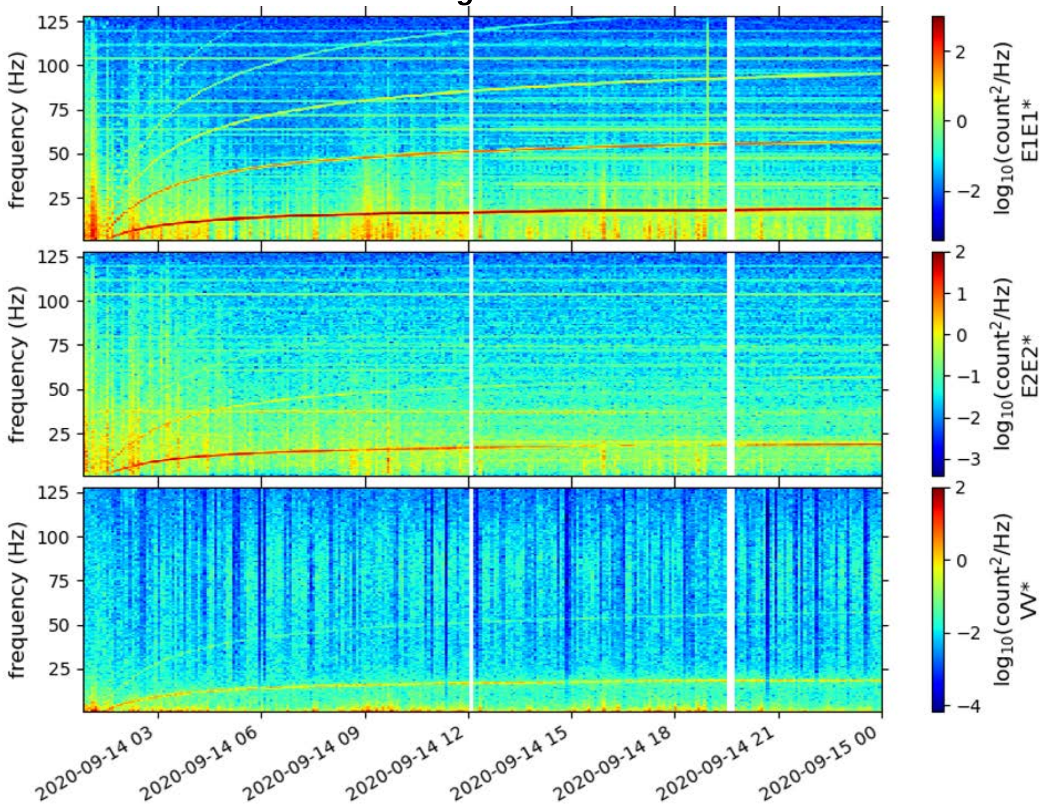

Figure 2.3.12

2.4 Electrostatic perturbations of the BIAS measurements

To be included in the next version of the document.

2.5 Focus on the “120 kHZ PCDU” perturbation

In this section we focus on the « 120 kHz PCDU perturbation ». Using the better frequency resolution of the TDS we identify statistically the various frequencies of the PCDU. We look also at the global power of the 120 Hz line and the coupling between the RPW antennas and the solar panels.

2.5.1 Individual frequencies of the « 120 kHz » pollution

On Figure 2.5.1 are displayed two different spectra, obtained by TDS, around the 120 kHz peak with two different frequency resolutions. While with the 130 Hz frequency resolution four distinct peaks are observed by TDS, it appears that the ~119 kHz peak is composed of three peaks.

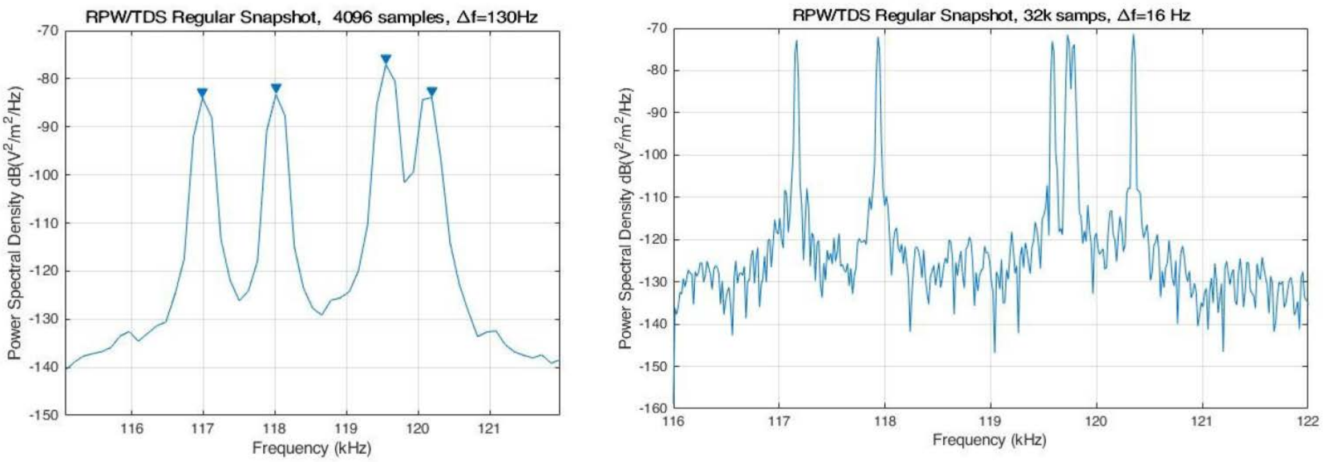

Figure 2.5.1

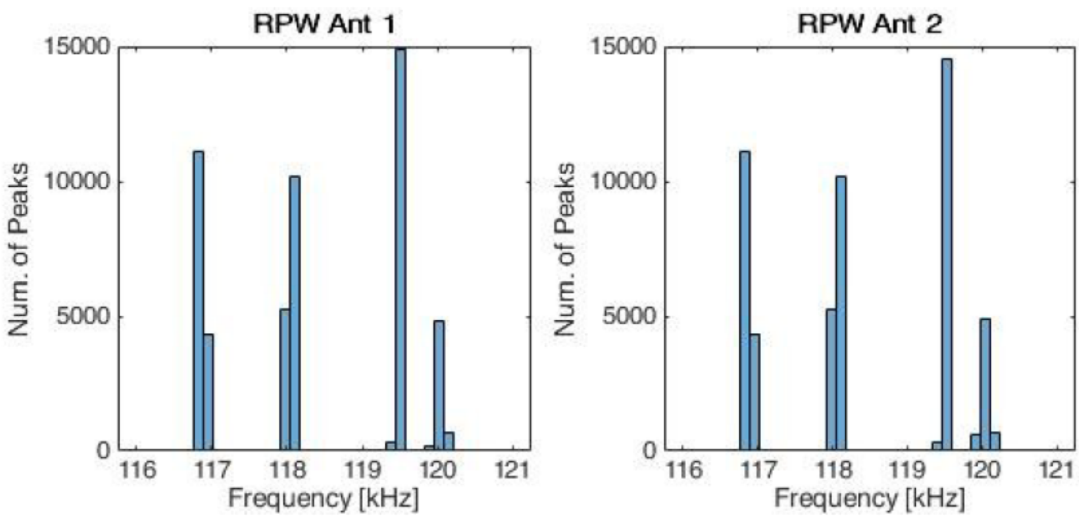

Figure 2.5.2

An automatic peak detection has been performed by the TDS team on data in monopole configuration for the the period Feb 25 – May 20 2020. Waveform snapshots of 4096 data points, sampled at 524 kHz, corresponding thus to a frequency resolution Δf=130 Hz, have been analyzed. Peaks with a power >15 dB above background have been detected. The histograms of the frequencies of these peaks fror Antennas 1 & 2 are displayed on Figure 2.5.2. A similar distribution of peak frequencies is also obtained for Antenna 3 but not shown.

Figure 2.5.1 show that the generic 120 kHz surious is actually composed of, at least, four individual spurious at 116.8, 118, 119.5 & 120 kHz. When observed by the TNR, which frequency resolution is Δf/f=4% at 3dB, these four spurious lines are observed as one single and large pollution line as can be seen on Figure 2.5.3.

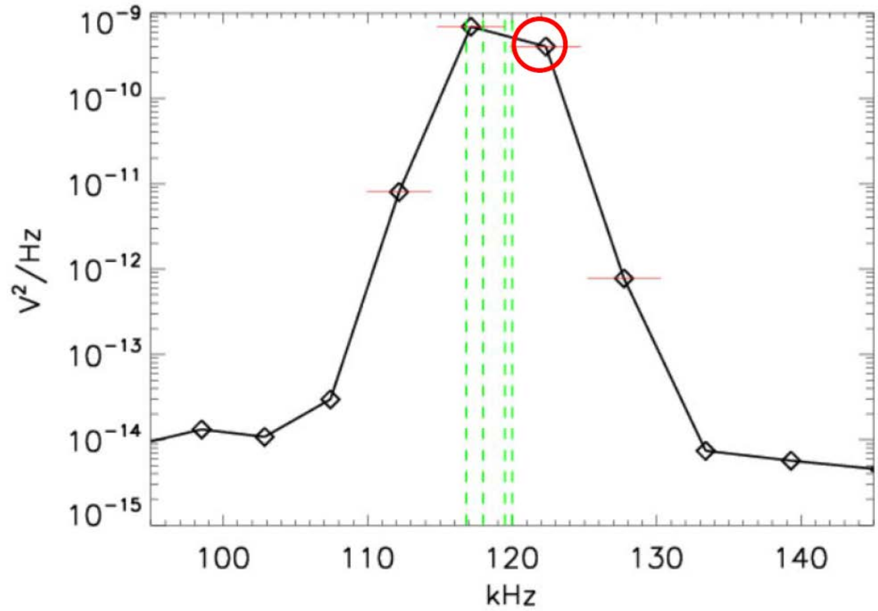

Figure 2.5.3 : TNR spectrum of the 120 kHz PCDU spurious. Overplotted with vertical green dashed lines, le 4 individual spectral lines as detected by the automatic peak detection applied on the TDS dats (see text for more details).

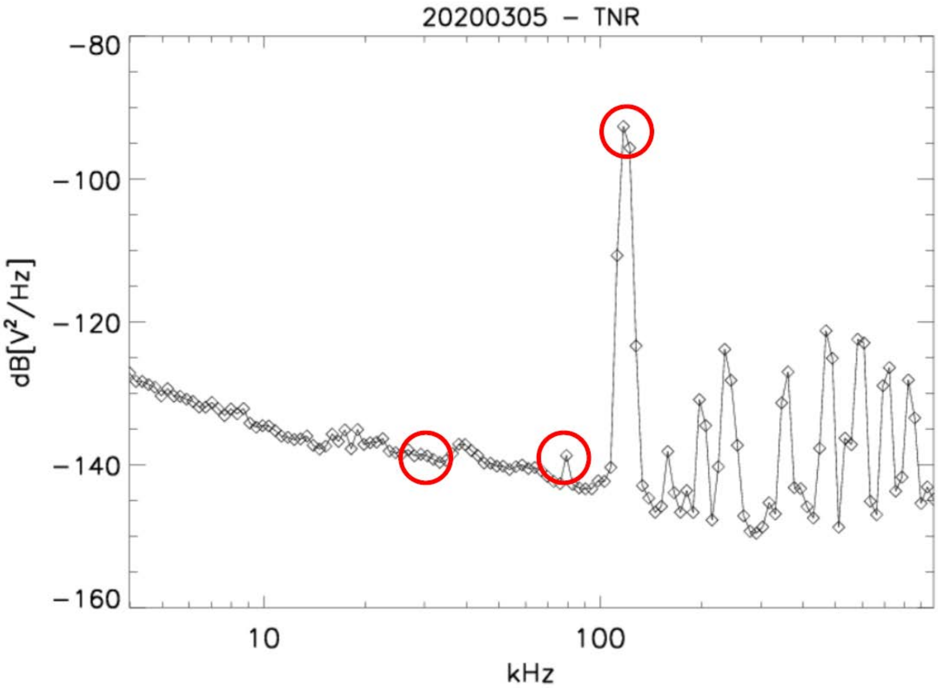

Figure 2.5.4

2.5.2 Time variation of the « 120 kHz » power

A simple examination of all the TNR daily summary spectrogram reveals that the « 120 kHz » perturbation is **always** present in the RPW data. Eleven consecutive days of TNR data have been displayed on Figure 2.5.5. Power spectral densities (converted in dBs) have been displayed for three different TNR frequencies which are indicated by the red circles on Figure 2.5.4. These frequencies are 41.414, 82.827 and 122.322 kHz. As can be seen on Figure 2.5.5

the perturbation at 120 kHz is always present with an average power around -96 dBs, about 50 dBs above the background signal in this frequency range. Note also that the temporal variations of the power at the three chosen TNR frequencies seem to be similar. The reason for this behaviour is still under investigation.

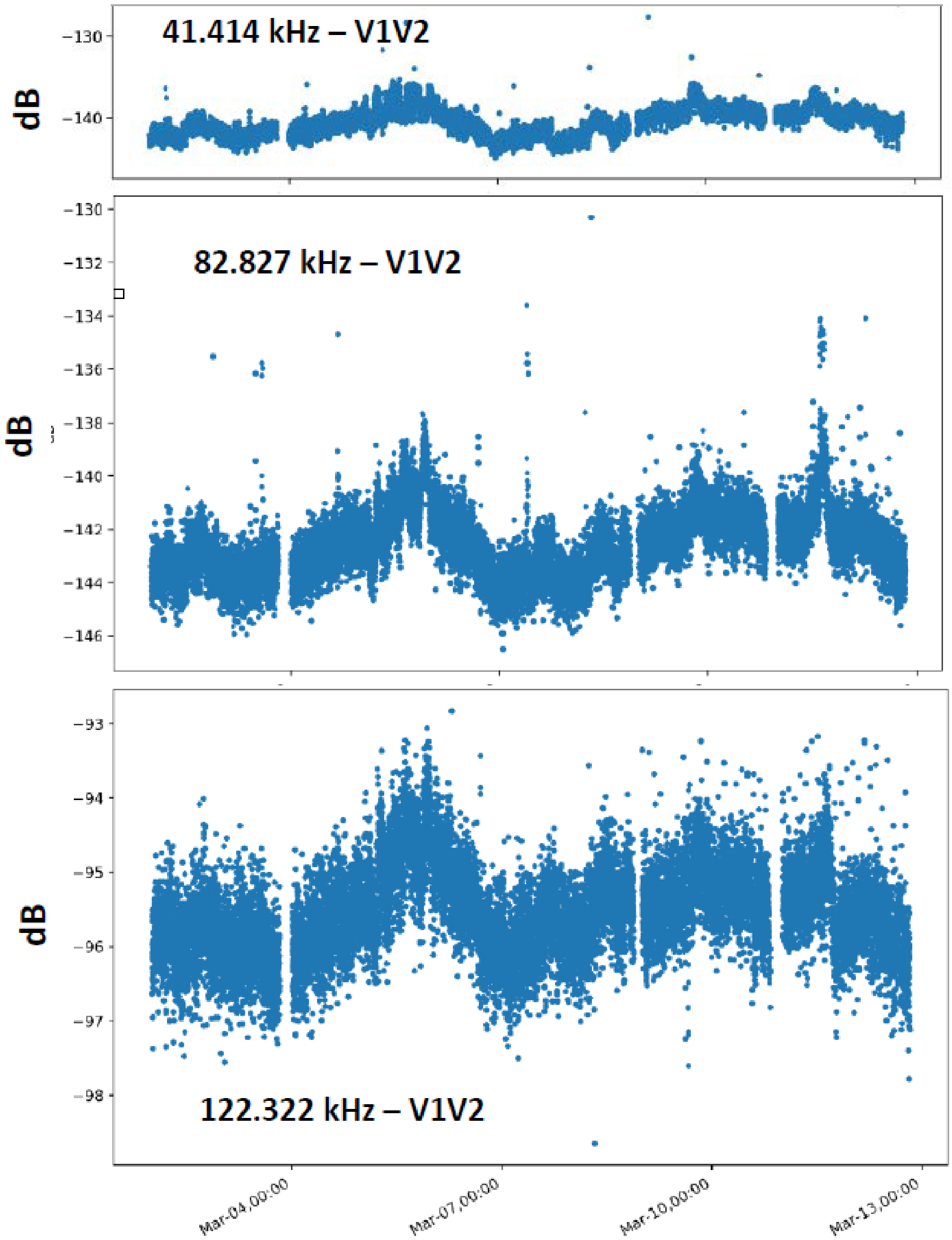

Figure 2.5.5

2.5.3 Coupling with the solar panels

In order to fully demonstrate that the 120 kHz perturbtion seen by RPW is from S/C origin and is emitted by the solar arrays (SA), we have investigated the the coupling between the SA and the RPW antennas. We have looked for any variation in the 120 kHz power related to the SA rotation which occurred during the NECP. The table below indicates the times of these different rotations.

DoY	Date	Solar Array Rotations
91	31/03/2020	from 0 to 30 degrees @11:17:28 (300s)
120	29/04/2020	from 30 to 56 degrees @00:47:03 (300s)
127	06/05/2020	from 56 to 60 degrees @~19:52
152	31/05/2020	from 60 to 70 degrees @~20h30
181	29/06/2020	from 70 to 60 degrees @~18h55 (TBC)

For any single rotation there is a change in the power in the *120 kHz* line as observed by TNR. For instance on Figure 2.5.6 we have displayed the variation of the power at 117 and 122 kHz, around the time of the steering of the solar arrays from 30° to 56°.

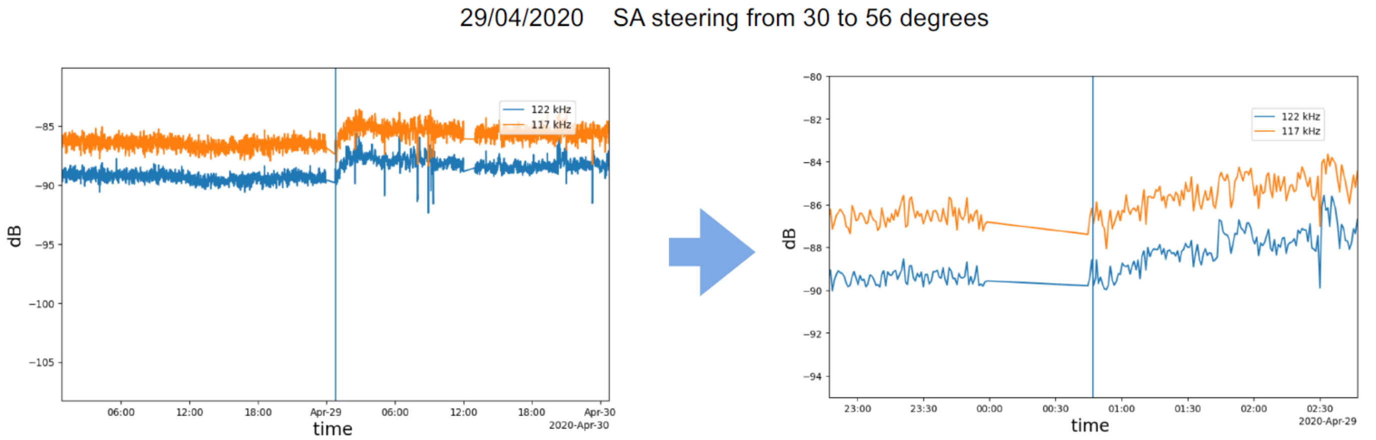

Figure 2.5.6

On Figure 2.5.7 we have plotted the averages and standard deviations of the power at 117 kHz for entire days of measurements for which the orientation angle is given by the abscissa. There is a clear trend on this Figure

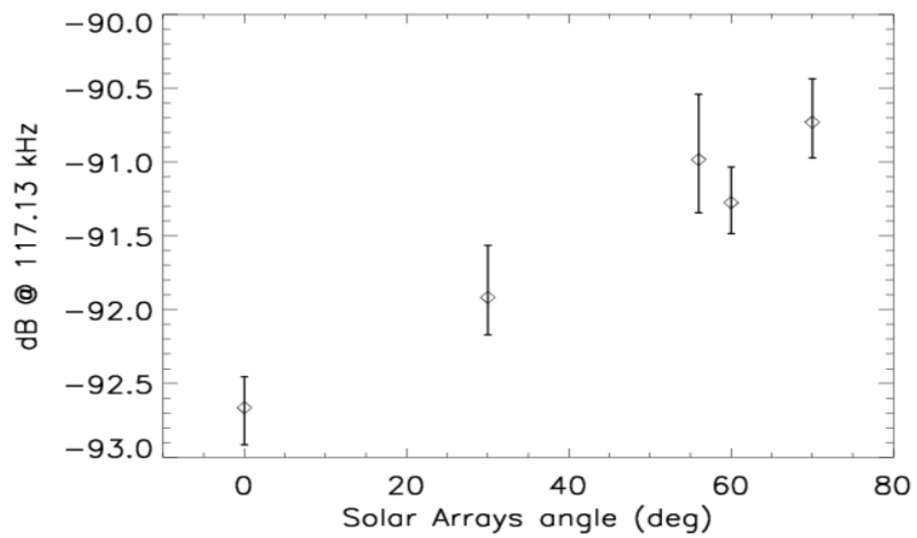

Figure 2.5.7

2.6 Analysis of the "RPW EMC campaign" on June 02/03 2020

2.6.1 TNR-HFR

At the time of writing the report and after a visual inspection hourly TNR-HFR dynamic spectra for these two days we do not see any extra perturbation (to the already know platform spurious and harmonics) which would come from some payload system. If they exist during this EMC campaign, these perturbations are hidden by the strong platform perturbations.

We however need to perform a more detailed automatic search to check whether there is still some weak perturbations present in the data.

2.6.2 TDS

No noticeable perturbation, that would come and go with the instrument activity, has been observed for TDS during the campaign. The only perturbation which was observed is a very faint 250 kHz emission which is sporadic. This could be some heater, but its signal is so weak that it Does not matter

2.6.3 LFR

The LFR sub-system is the only one for which additional EMC perturbations coming from specific payload activities have been observed during the June 2020 campaign. The Figures 2.6.1 and 2.6.2 below displays some magnetic perturbations from the Solo-HI instrument (at ~6.3 kHz) and the EUI instrument (broadband noise).

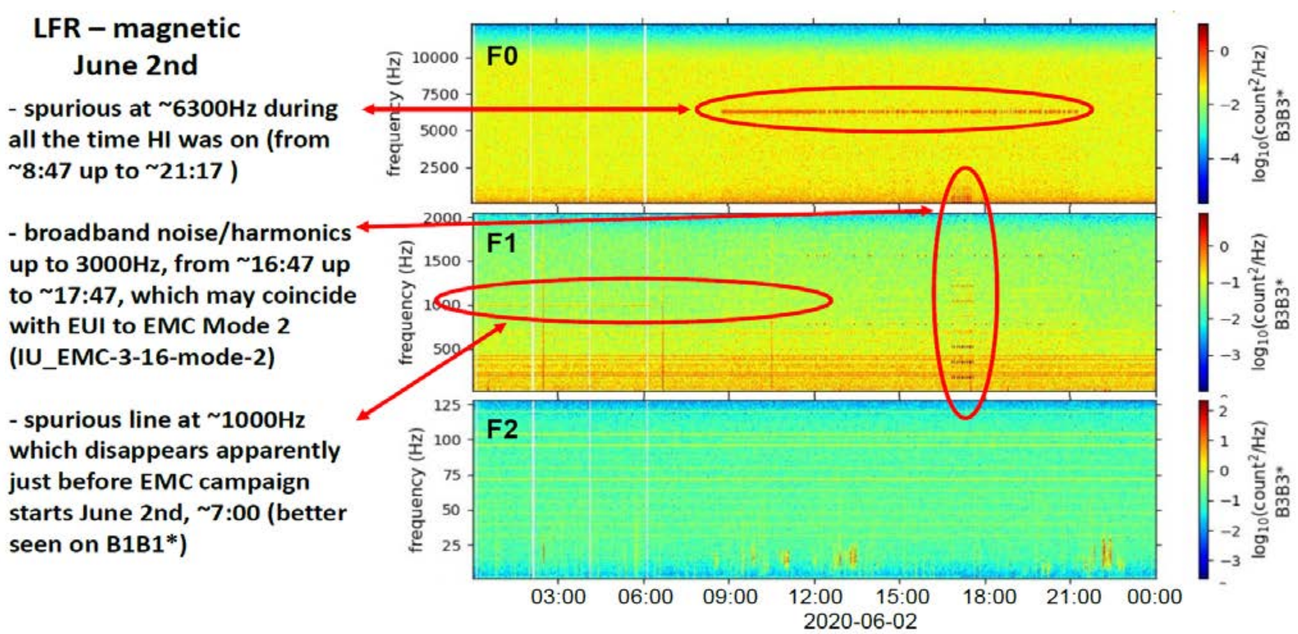

Figure 2.6.1

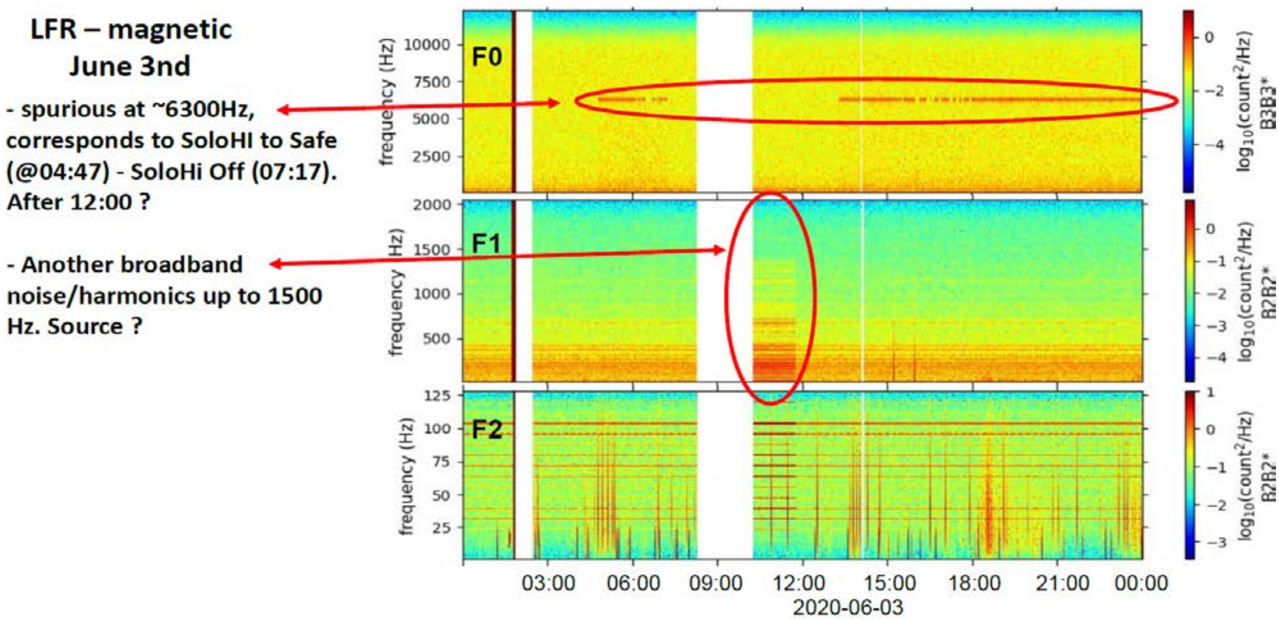

Figure 2.6.2

As for the electric perturbations, no obvious perturbations associated to the operations of other instruments has been noticed.

3 THE IMPACT ON THE SCIENCE AND POTENTIAL MITIGATIONS

3.1 Impact on TNR-HFR and possible mitigations

As can be seen on Figures 2.1.3 and 2.1.4, in the TNR range about 40 frequency channels, out of 128, are corrupted by the 80 kHz and 120 kHz S/C perturbations and their harmonics. This is unfortunately a large number. In the HFR frequency range, the situation is even worse. Only about 40 frequencies, out of 320, does not seem to be perturbed by the above perturbations. A detailed analysis of HFR data from Figure 2.1.3 shows that only about 40 frequency channels have signals which reach the galactic background.

On the other hand, the above situation does not mean that the corrupted frequencies, except the 120 string peak, cannot be used for science at all. They can be used for extremely strong Type III bursts for which the natural radio signals are well above the perturbations. This is the case for maybe 10 to 20% of the expected Type III bursts. For the science related to the solar radio emissions, we are losing frequency resolution and dynamic range. Globally the impact on the TNR-HFR science is about xx % as detailed in section 5.1.

As far as the mitigations are concerned and since nothing can be done in this area by the S/C, we have started to filter the corrupted frequencies on the ground data. Figure 3.1.1 shows an example of such filtering. On this Figure, Raw TNR data (upper panel) and filtered TNR data (lower panel panel) have been displayed for 15-June-2020. On the raw data the 120 kHz has already been removed. All the harmonics are visible as horizontal lines. On the filtered data, the latter are removed and the plasma peak at ~50-60kHz is more pronounced. The filtering technique is based on an FFT of the radio power. Note also that the periodic signal at around 300 kHz is due to the S/C battery charging and should be minimize in further operations.

Another mitigation, which is possible in the TNR domain, would be to modify the digital analysis filters by reducing their bandwidth for the polluted frequencies. This is under investigation and will require a patch of the TNR flight software.

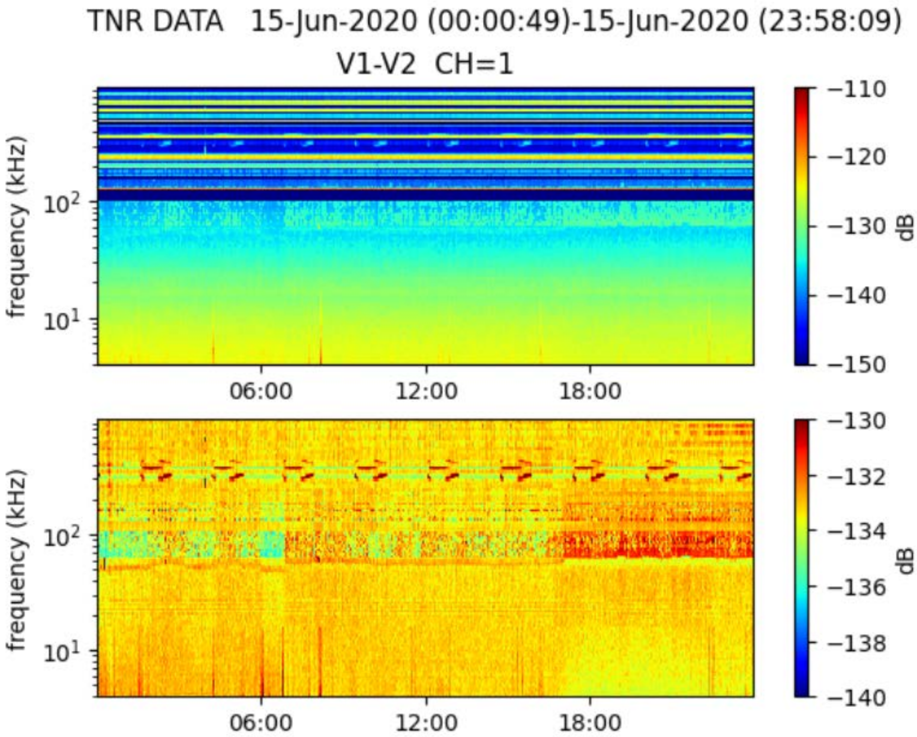

Figure 3.1.1

3.1.1 Impact on the RPW Low Latency data

There are two Low Latency data products for RPW

- The plasma frequency detected onboard by a plasma peak tracking algorithm
- The 1 MHz radio flux

As one could expect, the internal TNR-HFR plasma peak tracking software is detecting all the time the PCDU *120 kHz* peak as being the plasma frequency. Also, the power at 1 MHz, which is obtained from the calculation of median power of the the last 5 TNR frequency is probably corrupted by the 8th harmonic of the 120 kHz. On Figure 3.1.2 we display a comparison with the Type III observed on June 6th and which is only visible after some data cleaning. This Type III is not visible on the Low Latency 1 MHz flux.

3.1 Impact on TDS and possible mitigations

The numerous interference lines observed by TDS increases the baseline level of the instrument, making it more difficult to observe weaker signals, in particular in monopole mode. Fortunately, in a dipole mode, the remaining interferences are much less numerous.

Specifically, the stable and very narrow interferences at 15.3, 80, 100, 127, 160 and 200 kHz can be effectively filtered by digital post-processing and due to their low amplitude have little to no impact on the science.

Unfortunately, the same is not true for the PCDU emission, which consists of up to 6 spectral lines spanning the interval between 117 and 121 kHz. This part of the spectrum essentially unusable so any natural emissions in this range cannot be seen. We can filter this out of the waveform, but the loss of information is significant and the filtering of the time series will also affect frequencies adjacent to this range.

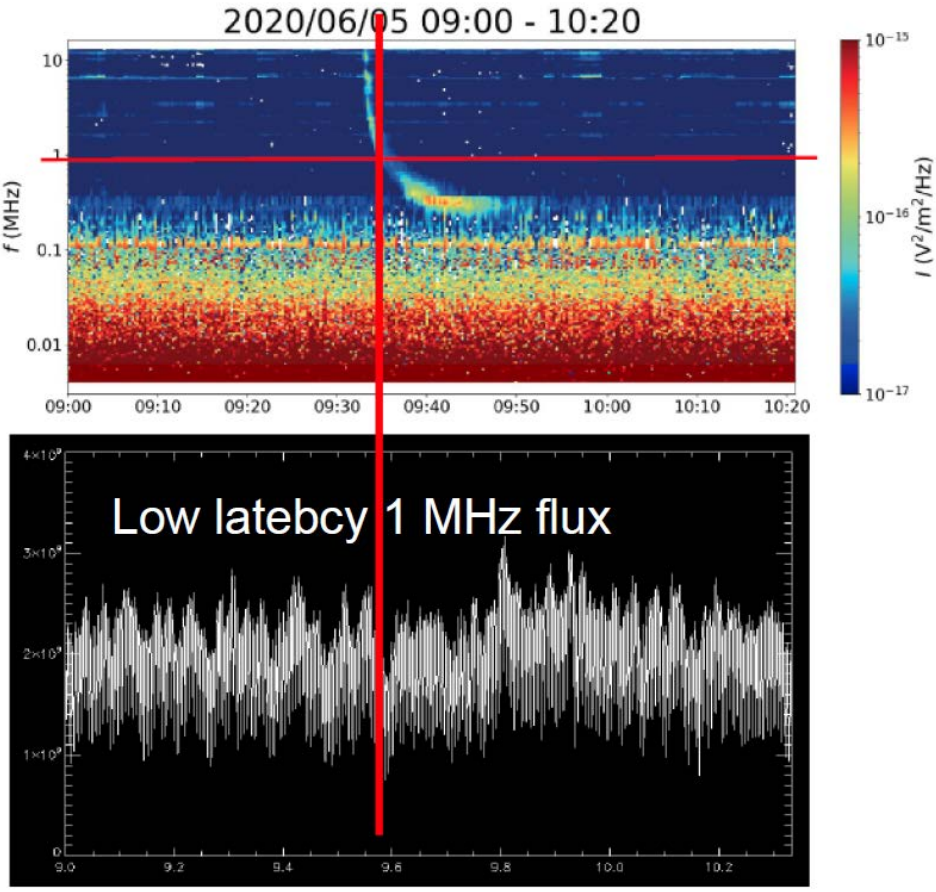

Figure 3.1.2

The most critical issue is that the artificial signal from PCDU interferes with the capability of TDS to perform on-board detection of natural waves and dust impact. The narrowband interference resembles natural waves and the detection algorithm is effectively blinded by this artefact.

TDS samples nominally either at 262 ksps or 524 ksps. When sampling at 262 ksps, the anti-aliasing filter can be adjusted (on board) to damp the 120 kHz emission, which is already in the stop-band of the measurement. This allows for the detection algorithm to work with some configuration updates. The measurements in the 262 ksps mode and in particular on a dipole configuration are therefore more or less acceptable.

A worse situation is when TDS operates in the 524 ksps mode, which is need for the perihelion passes. Here the 120 kHz interference is in the middle of the frequency band. This needs to be filtered out from the data on ground with the loss of data discussed above, but the current flight software cannot account for this in the detection algorithm. A TDS flight software patch is necessary to correct this. This new version of software is planned for late 2020.

3.2 Impact on LFR and possible mitigations

Most of the numerous spurious signals observed by LFR are more or less weak and will impact the observation of weak signals. If avoiding the emission of these signals may not be possible a characterization of them is still needed in term of their origin, condition of occurrence and variability. Lines and harmonics becoming stronger during the mission (as noticed at 20-40Hz for electric field measurements) may be filtered out from the onboard spectral products, if they are stable. The precise impact on the LFR observations is thus still being assessed.

3.3 Electrostatic impact on the BIAS measurements and possible mitigations

To be included in the next version of the document.

4 LESSONS TO BE LEARNED BY ESA

The issue of the PCDU filtering was raised by the RPW team **very early** at the beginning of the project. This early request has been made in light of the experience gained on the NASA STEREO project for which a radio receiver, with similar performances than the TNR-HFR, has been developed by the RPW PI institutes. This request has even been recorded in the minutes of the EMC Meeting Working Group Meeting #6 [RD2], where on page 10 it is written:

PCDU filtering: Astrium (FHN) are currently analysing the interaction between the PCDU and the solar arrays. This analysis is a variation on the analysis carried out for the BepiColombo **project but with modifications appropriate for Solar Orbiter. The results will be used to determine whether a filter is needed and if so, the characteristics of the filter.**

In addition, a specific meeting entitled « EMC Lessons Learned from STEREO », was organized, on the request of the RPW PI, at the Paris Observatory on 10 January 2013. John.Aulton from Airbus Defense and Space (at that time Astrium/EADS) participated to this meeting.

Unfortunately, and despite numerous warnings, the ESA project has always refused to implement a dedicated band-pass filter between the PCDU electronic box and the solar arrays. the result of this refusal is unfortunately materialized with the spurious emission at 120 kHz. Hopefully such a mistake will not occur on the ESA JUICE mission, which will carry a radio receiver similar to the TNR-HFR.

5 GENERAL CONCLUSIONS AND CONSEQUENCES FOR THE SOLAR ORBITER SCIENCE OPERATIONS

The impact of the patform at “120 kHz”, throught the solar panels has been clearly established. This pollution is is composed of 4 main frequencies 116.8, 118, 119.5 & 120 kHz.
There is nothing which can be done at S/C level to mitigate this perturbation. The only mitigations will have to be implemented by the RPW team either by post-processing of the data or by forthcoming changes in the RPW flight software.

5.1 Summary of the EMC perturbations on RPW

The table 5.1 below summarizes all the perturbations observed and characterized so far.

label & description	corrupted frequencies	sensor E/B	root cause	impacted sub-systems	severity & mitigations
#1: AOCS Synchronization Pulse	8 & 16 Hz	B	S/C AOCS	LFR	low severity
#2 : LF 3 hours periodicity perturbation	≲ 500 Hz	B	unknown	LFR	TBD
#3: SCM heater	≲ 100 Hz	B	SCM	LFR	low severity, mitigation by flagging the data
#4: 36 Hz & harmonics	≲ 200 Hz		unknown		medium severity
#5: Solo-HI 6.3 kHz	~ 6.3 kHz	E & B	Solo-H1	LFR	medium severity. Should be taken care by ESA during operations
#6: EUI science mode	Broadband up to 1.5 kHz	E & B	EUI	LFR	medium severity. Should be taken care by ESA during operations
#7: 80 kHZ	~80 kHz and many harmonics	E	S/C Reaction Wheels electronics	TNR-HFR	high severity. Mitigation by RPW
#8 : 120 KHz	~120 kHz and many harmonics	E & B	S/C PCDU noise radiated by the SA. Root frequencies are	TNR-HFR & TDS	high severity. Mitigation by RPW
#9: ~250 kHz	244.6 & 255.5 kHz	B	Mag heater	TNR	Low severity, mitigation by flagging the data
#10: ~300kHz	Several frequencies around 300 kHz	E	S/C battery charging	TNR	high severity if not mitigated by ESA during operations.

Table 5.1

5.2 Global science impact

Following the Table 5.1, providing the severity of the pollutions, and the annex, providing the amount of science return for each sub-system, we summarize in the Table 5.2 below the science impact of the EMC perturbations.

We have assigned empirically 5%, 10% and 15% impact for low, medium and high severity EMC impacts. These numbers are somehow overestimates since the same science impact is sometime from two different EMC perturbations. On the other hand, the final EMC impact is somehow underestimated since the impact on the BIAS science is still being assessed and does not appear right now in Table 5.2.

Anyway, if we assume that EMC#10 will be mitigated in future operations then the global EMC impact on the science is of the order of 20-25 %.

	BIAS	LFR	TDS	TNR-HFR	
science	**21,00%**	**30,00%**	**22,00%**	**27,00%**	**100,00%**
EMC #1		5,00%			
EMC #2					
EMC #3		5,00%			
EMC #4		10,00%			
EMC #5		10,00%			
EMC #6		10,00%			
EMC #7				15,00%	
EMC #8			5,00%	15,00%	
EMC #9				5,00%	
EMC #10				15,00%	
Total EMC impact (EMC#10 excluded)		**40,00%**	**5,00%**	**35,00%**	
Total science impact (EMC#10 excluded)		**12,00%**	**1,10%**	**9,45%**	**22,55%**
Total EMC impact		**40,00%**	**5,00%**	**50,00%**	
Total science impact		**12,00%**	**1,10%**	**13,50%**	**26,60%**

Table 5.2

6 ANNEX: SCIENCE DISTRIBUTION FOR THE VARIOUS SUB-SYSTEMS

science objectives	BIAS	LFR	TDS	TNR/HFR	
Interplanetary Shocks, Magnetic Reconnection, and Current Sheets,					
Identify and characterize the solar wind reconnection physics in current sheets with thickness down to the ion scales and smaller.	35	45	10	10	100
Resolve interplanetary shock field and plasma structure down to the spatial and temporal scales comparable and smaller than the typical ion scales.	35	45	10	10	100
Measure the relative strength of the convection vs cross-shock electric field as a function of heliospheric altitude.	35	45	10	10	100
Compare microphysics of solar wind reconnection with magnetospheric reconnection.	35	45	10	10	100
Solar wind Microphysics, Turbulence, and Heating					
Identify and characterize the waves associated with the plasma instabilities that isotropize and heat the solar wind	35	45	5	15	100
Identify and characterize the waves that create and isotropize the electron halo population	35	35	5	25	100
Measure the turbulence dissipation range and understand it scaling with heliospheric radius	35	50	5	10	100
Electron Density and Temperature from Quasi-Thermal Noise Spectroscopy					
Measure precisely both the electron density and temperature, with accuracies respectively of a few % and 10 %, at perihelion when the L > lD.	30	30	0	40	100
Characterize the non-thermal character of the electron distributions at perihelion.	10	20	0	70	100
Langmuir Waves and Electromagnetic Mode Conversion					
Measure for the first time in the solar wind both the electric and magnetic field waveforms at high frequency (up to 500 kHz).	5	10	70	15	100
Solve the problem of the mode conversion from Langmuir to electromagnetic waves using fields and density (spacecraft potential & thermal noise) measurements	10	40	20	30	100
Characterize the energy balance between electron beams, Langmuir waves and e.m. radio waves at several radial distances	5	15	50	30	100
Solar Coronal and Interplanetary Radio Bursts					
What is the role of shocks and flares in accelerating particles near the Sun?	20	30	20	30	100
How is the Sun connected magnetically to the interplanetary medium?	5	10	20	65	100
What are the sources and the global dynamics of eruptive events?	5	10	20	65	100
What is the role of ambient medium conditions on particle acceleration and propagation?	20	30	20	30	100
How do variations and structure in the solar wind affect low frequency radio wave propagation?	10	20	30	40	100
Interplanetary Dust					
detection of interplanetary dust and heliospheric mapping	0	0	60	40	100
	21	30	22	27	